Eur. Phys. J. Special Topics **192**, 121–128 (2011)

DOI: 10.1140/epjst/e2011-01366-6

THE EUROPEAN PHYSICAL JOURNAL SPECIAL TOPICS

Regular Article

Impact of electric fields on the speed of contact line in vertical deposition of diluted colloids

M. Giuliani[a,b], M. Pichumani[a], and W. González-Viñas[c]

Dept. of Physics and Applied Math., University of Navarra. Irunlarrea s/n, 31080 Pamplona, Spain

Received 21 January 2011 / Received in final form 25 January 2011
Published online 9 March 2011

Abstract. We report experimental results on the influence of electric fields on the contact line dynamics of the vertical deposition of water-based diluted colloidal suspensions. We measure the speed of macroscopically receding contact line for different initial concentrations and applied voltages. We explain the observed behavior *via* the electrophoretic effect in the region near the contact line. The electrophoretic effect induces a concentration gradient along the direction of the applied field which influences the morphology of the dried deposit of colloidal particles. Thus the applied field has an effect on the receding contact line through morphological formation and its transition.

1 Introduction

Colloidal phase transitions have been largely studied since they provide relatively easy models for hard condensed matter systems. These mesoscopic models are more realistic than an ensemble of macroscopic entities [1]. The transitions exhibited by these systems are technologically relevant due to the large number of possible applications (from filtering membranes to optoelectronic devices, including variety of sensors). In these systems, it is a major challenge to understand precisely the degree of involvement of the different processes that control the transitions. We believe that this understanding is the key to make such applications possible. Recently, methods like Laser Confocal Microscopy and Atomic Force Microscopy are employed at colloidal length scales, allowing precise characterization of the structures [2–4]. Visualization at particle level can be achieved from these methods which increase the interest of the community and the number of contributions towards the field [5–13]. Also, colloidal systems have many applications involving physics and engineering and specially, it is the fact that they allow

[a] MG and MP contributed equally to this work.
[b] *Present address:* Dept. of Phys., University of Guelph, Canada.
[c] e-mail: wens@fisica.unav.es

the formation of multi-scale structures, as they can be ordered at mesoscopic characteristic lengths. Additionally, the usefulness of these structures is maximum when they are dried (forming colloidal crystals, glasses or more complex structures).

Until now, the drying of colloids to well ordered (or, in general, structured) solids remains difficult. In most of the cases, this kind of process is called as evaporation-induced self-assembly [14] which involves a phase transition from the fluid suspension to the dried structure. When a non-equilibrium phase transition takes place, one of the most important parameters to consider is the time-scale at which the transition is occurring. But, for the equilibrium phase transition, at the given thermodynamic values, the longer the transition is, less defects are observed in the arriving phase. On one hand, in the latter kind, the process is too long to be useful in applications. On the other hand, the former transition could rely on other mechanisms (kinetic ones) that could provide the desired structures and sometimes with less defects. Nevertheless, these mechanisms usually increase the complexity of the systems and need to be studied in depth. A common approach to simplify this transition is to impose privileged directions (by means of external fields like gravitational, electric, magnetic, hydrodynamics or boundary conditions). All these experimental conditions aim to break some symmetries in the system.

The evaporative colloidal phase transition can be studied in several time scales depending on the rate of evaporation. On the long temporal scale limit, we have stable colloids that are evaporated slowly. This procedure is conceptually similar to the slow sedimentation of colloidal particles and the removal of the liquid [15–17]. Colloidal particles are highly influenced by the hydrodynamics present in the experimental system. Consequently, the process of removing the liquid phase remains critical and its effect cannot be neglected [18]. On the short temporal scale limit, we have quick transitions (from a few hundreds of seconds to less than a second) like in the spin-coating of colloidal suspensions, where the continuous phase is highly volatile [4,19,20]. In these transitions, the dynamics is important and it leads to orientationally ordered polycrystals. However, it is thought that it is not possible to achieve large crystallites [19]. In the mid range of temporal scales, we found techniques derived from Langmuir-Blodgett method [21–23]. In our previous experiments we have focused on the vertical deposition technique at a controlled temperature in order to optimize the deposition and to characterize the relevant parameters associated to it [24].

In vertical deposition of colloids, there are other important variables which need to be controlled in order to fabricate homogeneous colloidal crystals. Firstly, concentration; which is neither homogeneous nor constant along the whole experiment. Under certain conditions [25,26], particles accumulate near the contact line in a region called particle pool zone (PPZ). Thus, the structure formed depends on the local concentration in the PPZ, rather than on the initial concentration. Secondly, the importance of flows, which are large and of different nature: Marangoni flows due to evaporation, the capillary flows due to the predeposited structure (thus making the system dependent on its previous history), and other flows (convective-like). Also, it is important to consider the hydrodynamic interactions between the particles [27].

In this paper, our aim is to deepen the understanding of some of these phenomena in the vertical deposition process by applying a weak DC field, comparing to the previously studied situation with the absence of electric fields [25]. We characterize the speed of contact line as the fluid phase evaporates and the colloidal structure is deposited. The applied electric field has an effect on the colloidal suspension *via* electrophoresis, which increases or decreases the particle concentration near the depositing zone.

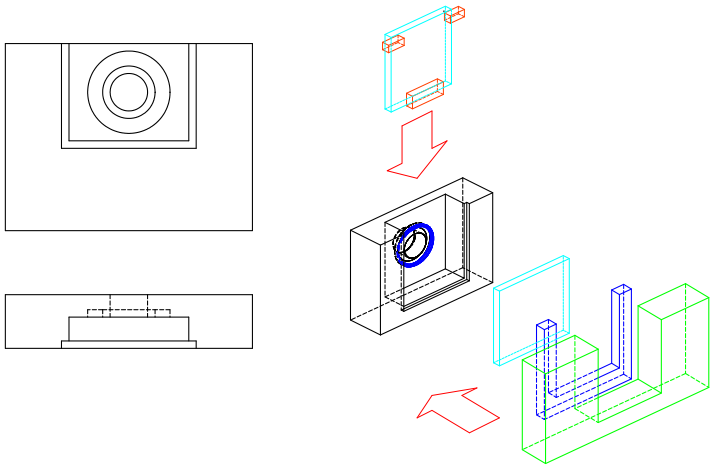

Fig. 1. Sketch of the used cell. Left: orthogonal projected front and top views of the main body. Right: isometric exploded view of the ensemble that conforms the experimental cell. Web version: Different parts of the cell are colour coded: black – main body; cyan – ITO substrates; blue – rubber sealing; orange – ceramic spacers, green – compressing frame.

2 Experimental setup and procedure

Colloidal dispersion of polystyrene spheres (diameter = 1.3 μm, polydispersity = 0.039, surface charge ~ -7 μC/cm^2) suspended in water were acquired from Dr. Paulke at Fraunhofer-IAP, Germany. We dilute this stock suspension to the desired concentrations with ultra pure water. For the experiments, we used three initial concentrations: 0.1%, 0.3% and 0.5%. All the concentrations are expressed in w/w units. The experiments were performed in a chamber at fixed temperature and humidity (63 °C, below 2%RH respectively). A detailed explanation of the substrate preparation and the experimental setup can be found in previous works [25,28].

In Figure 1, we present the schematic design of the cell. We built the main body (Figure 1 – left) with Teflon®. It gives support to other elements which conform the cell. One face of the substrates (17×18 mm^2 standard glass pieces) is coated by a thin layer (150 nm) of Indium Tin Oxide (ITO). This conductive face is in direct contact with the suspension and it allows to apply electric fields with an optimal geometry. Substrates are kept parallel to each other and are separated by 1 mm ceramic spacers. Two rubber seals are compressed by a metal frame to provide the necessary robustness and to avoid leaks.

Constant electric fields of the order of 1 V/mm are applied perpendicularly to the conducting substrates. We monitored the electrical current which passes through the suspension to check that the current remains constant through out the experiment. The rear part of the deposition cell is illuminated by means of a cold light source in order to image the contact line. The receding contact line was captured by a CMOS camera. We extract the position of the contact line as a function of time from which the speed of the contact line is obtained.

3 Results

We report the characteristic speed of the contact line at different initial concentration and applied voltages. For each experimental condition, we obtain the cumulative distribution of the measured speeds during all the deposition. The characteristic

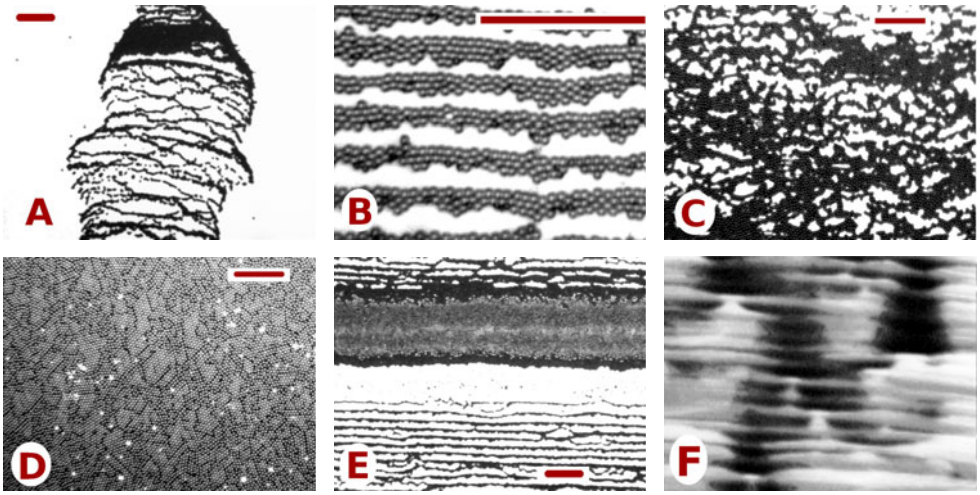

Fig. 2. Optical micro-graphs of the several morphologies of the dried deposits of colloidal particles. A – Vertical sparse stripes (VSS) at 0.1%, B – Non compact morphology (NC) at 0.3%, C – Non compact dense morphology (NCD) at 0.5%, D – Compact monolayer (CM) at 0.5%, E – Multilayer (ML) followed by sparse deposit at 0.5%, F – Vertical column multilayer (VCM) at 0.5% (width of image is 6 mm). Scale bars are 25 μm and the magnifications are different.

speeds are calculated by fitting Gaussian distribution functions to this cumulative distribution. The number of used Gaussian distribution functions are varied to get a proper fit. Typically not more than two functions were necessary. Subsequently, we associated each characteristic speed to the mean of each Gaussian distribution function. Its error is the error of the fit. The used concentrations give multiple morphologies ranging from a sparse sub-monolayer (at 0.1%) to a multilayer deposit (over five particle diameters in thickness at 0.5%). The thickness has been estimated from the step-wise intensity profile when the thickness increases slowly from a monolayer. A summary of the structures is shown in Figure 2, where the images are arranged in such a way that the number of particles per unit area increases from left to right (first row of Figure 2: A, B and C). In all the cases, the white area is the bare substrate and the dark regions are the deposited particles. In Figure 2, morphology A shows particles organized in a column-like arrangement, and the column is of very sparse sub-monolayer deposit. In the next morphology (B), the columns have widen enough to form a similarly sparse deposit which expands over the surface of the substrate. These deposits are typical for low concentration experiments (0.1% and partially to 0.3%). The following morphology (C) still shows a sub-monolayer deposit extended over the substrate but the number of particles per unit area had increased. The next structure (D) is a compact monolayer, where the surface coverage on the substrate reaches its maximum. Structures with more particles per unit area are multilayer deposits (E). Typically at higher concentrations, structures with higher particle density were found. In some situations, these structures arrange themselves in vertical columns like structures as seen in Figure 2 – F, called Vertical Column Multilayer (VCM).

Figure 3 shows the characteristic speed of the contact line for initial concentrations 0.1%, 0.3% and 0.5% at different applied voltages. Despite the small change in the initial concentration, the effect of the voltage on the characteristic speeds can be seen. The vertical axis values for concentrations 0.3% and 0.5% are different from 0.1% for

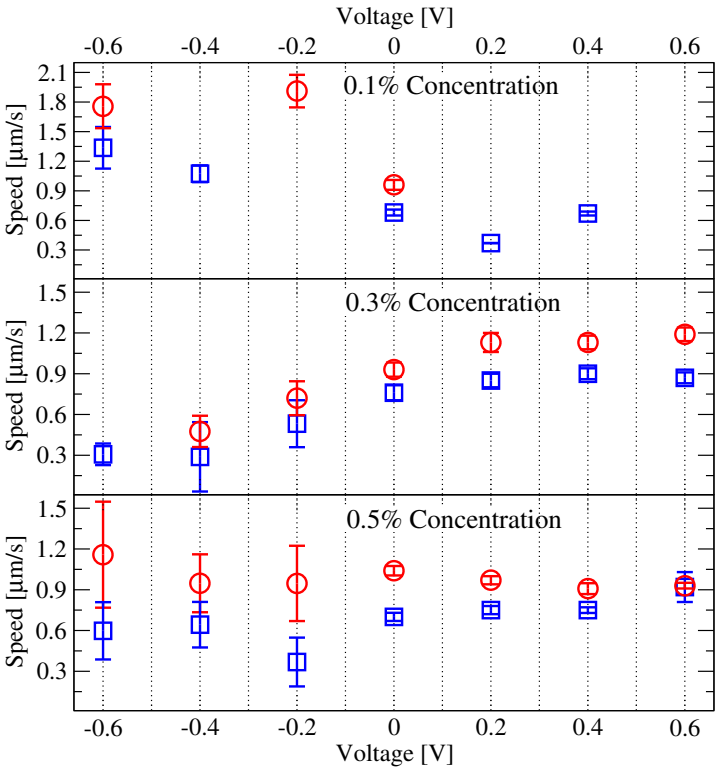

Fig. 3. Characteristic speeds of the contact line for each initial concentration at different applied voltages. For a given condition, in most cases, two characteristic speeds were measured (squares and circles).

better visualization. For the same experiment (at an initial concentration and at an applied voltage), two different characteristic speeds for the contact line (circles and squares) were measured, through analysis of gaussian fits, as it is explained above. As it will be shown below, they may correspond to different (local) conditions at the meniscus. At lowest concentration (0.1%), a decrease in voltage increases the characteristic speed of the contact line (squares) and in some experimental conditions, an additional speed is measured (circles, Figure 3 – Top). If we increase the concentration to 0.3%, the characteristic speeds of the contact line (both circles and squares) remain almost unchanged in the applied positive voltage region. But they decrease as the voltage decreases (Figure 3 – Center). Typically, a different behavior is observed at higher concentration (0.5%) where the two characteristic speeds overlap at 0.6 V and they diverge towards 0 V. For the applied negative voltage, the characteristic speeds remain constant within the error. (Figure 3 – Bottom). Large error bars are due to the fact that the different regions of the contact line are connected through surface tension. Consequently, bare speeds (those which might occur in homogenous local conditions for all the contact line) are perturbed by the surrounding regions.

4 Discussion and conclusions

On one hand, for a structure to form on the vertical substrate, it is necessary to have the particles available near the receding contact line. That is, to have a populated

particle pool zone (PPZ). Also, there is a dependence on the type of structure that has already been deposited: normally a forming multilayer increases the capillary flows due to its porosity and thus, a multilayer usually grows faster since the flows that drive particles toward the structure are larger. On the other hand, in our experimental conditions, Reynolds (Re) number is of the order of 10^{-6}. As the dispersion is density matched, the colloidal particles behave as inertial ones, and they approximately follow the flow. The capillary (Ca) number is of the order of 10^{-8}. Consequently, capillary forces are stronger than viscous ones.

The electric field may interact with the particles through several electrokinetic phenomena and with the fluid through the electrowetting effect. From the several electrokinetic mechanisms [29], electrophoresis is the strongest since it is related directly to the charge of the particle. We estimate that the electrowetting effect [30] induces a maximum change of 1% in the contact angle. The magnitude of this change lead us to consider the electrophoretic effect as the main consequence of the applied electric field. Moreover, the electrophoretic effect has been proved as an efficient electrokinetic mechanism in transporting colloidal particles [31,32]. We estimate that the electrophoresis in our experiment can result to an initial redistribution of particles in the direction of the field at a temporal scale of around 100 seconds. This gives a change in the concentration of the PPZ (corresponding to an increase in the positive electrode and to a decrease in the negative one).

Summarizing the mechanisms, the characteristic speed can be modified through: (i) Variation of the particle concentration in the PPZ [25,26]. (ii) Different types of deposited structures, which tend to grow at different characteristic speeds. Usually, multilayer (ML) and non compact dense (NCD) structures have higher speed of contact line than compact monolayer (CM) and non compact (NC) structures [25].

At low concentration 0.1% (Figure 3 – Top), in the positive voltages region, we do not observe a significant effect in the speed of the contact line. Furthermore, all the morphologies observed in these cases are similar. This suggests that the increase of concentration near the deposition region due to electrophoresis is not enough to give rise to more dense structures (NCD and ML). In the negative voltage region, we have a largely depleted PPZ. Regarding the deposits, we observe low density structures in a columnar arrangement (Figure 2 – A). This indicates that the decrease of concentration does not result in a further decrease of the density of the structure but into a morphological transition towards columnar deposits. These columns were not observed before [25] and they seem to be associated to larger growth speed.

At higher concentration, the growth speed shows a dependence with the applied voltage (Figure 3 – middle and bottom). Regarding the observed structures, in all cases we observe all the type of structures previously defined: ML and NCD (that tend to grow at faster rates), and CM and NC (that tend to grow at lower rates). However, we observe an increase of multilayer deposits (particularly in a columnar arrangement, see Figure 2 – F) as we increase the voltage and the concentration. That is, an experiment done at higher voltages and larger concentration results in an increase of vertical column multilayer (VCM).

For 0.3% concentration, in the negative voltage region, we observe a decrease of the growth speed as we decrease the voltage (Figure 3 – Middle – left side). This can be explained through a depletion of the PPZ induced by the electrophoretic effect on the particles. Given that the kind of deposited structures is maintained, their growth speed should decrease. In the positive voltage region, we obtain a saturation in the speed (Figure 3 – Middle – right side). From this, we observe that a larger concentration in the PPZ (induced by the electrophoretic effect) does not result in an increase of the speed. Instead, we observe that the area covered by the multilayers increases. Thus, the larger concentration results in thicker deposits where the additional particles are deposited.

At a concentration of 0.5%, the negative voltage region shows similar growth speeds to the positive region in the 0.3% case. The concentration in the PPZ will decrease due to the field effect, thus both experimental conditions could be comparable (positive region of 0.3% and negative region of 0.5%). For the positive region, the higher characteristic speed decreases slightly, while the lower one increases until they overlap at 0.6 V. The deposits observed are of growing complexity with alternating columnar structures (see Figure 2 – F). The simultaneous formation of morphologies with different growth rate could affect the characteristic speeds leading to the observed overlap.

In conclusion, we observe that an increase in the PPZ concentration (induced by an increase in the electrophoretic effect) results in a smooth transition from low growth speeds (at 0.1% from 0 V to 0.4 V) to high growth speeds (at 0.3% from 0.2 V to 0.6 V and at 0.5% from −0.6 V to 0 V, approximately). We found that the transition occurs in the region of applied negative voltage at 0.3% concentration. The extreme cases corresponding to very low concentration in the PPZ (low initial concentration and high negative voltage) and high concentration in the PPZ (high initial concentration and high positive voltage) require further microscopic studies [33].

This work is partly supported by the Spanish Governement Contract No. FIS2008-01126 and by the Gobierno de Navarra (Departamento de Educación). M.G. and M.P. acknowledge financial support from the “Asociación de Amigos de la Universidad de Navarra”.

References

1. L. Bragg, J. Nye, Proc. R. Soc. London **190**, 474 (1947)
2. L. Shereda, R. Larson, M. Solomon, Phys. Rev. Lett. **101**, 16 (2008)
3. D. Derks, Y.L. Wu, A. van Blaaderen, A. Imhof, Soft Matter **5**, 1060 (2009)
4. M. Giuliani, W. González-Viñas, K. Poduska, A. Yethiraj, J. Phys. Chem. Lett. **1**, 1481 (2010)
5. A. Yethiraj, A. van Blaaderen, Nature **421**, 513 (2003)
6. A. Yethiraj, A. Wouterse, B. Groh, A. van Blaaderen, Phys. Rev. Lett. **92**, 058301 (2004)
7. K. Lin, J. Crocker, V. Prasad, A. Schofield, D. Weitz, T. Lubensky, A. Yodh, Phys. Rev. Lett. **85**, 1770 (2000)
8. C. Murray, Annu. Rev. Phys. Chem. **47**, 421 (1996)
9. E. Weeks, J. Crocker, A. Levitt, A. Schofield, D. Weitz, Science **287**, 627 (2000)
10. H. Bodiguel, F. Doumenc, B. Guerrier, Eur. Phys. J. Special Topics **166**, 29 (2009)
11. H. Bodiguel, F. Doumenc, B. Guerrier, Langmuir **26**, 10758 (2010)
12. G. Berteloot, C.T. Pham, A. Daerr, F. Lequeux, L. Limat, Europhys. Lett. **83**, 14003 (2008)
13. K.Q. Zhang, X.Y. Liu, J. Chem. Phys. **130**, 184901 (2009)
14. C.J. Brinker, Y. Lu, A. Sellinger, H. Fan, Adv. Mater. **11**, 579 (1999)
15. K. Davis, W. Russel, W. Glantschnig, J. Chem. Soc. Faraday Trans. **87**, 411 (1991)
16. H. Míguez, F. Meseguer, C. López, A. Mifsud, J. Moya, L. Vázquez, Langmuir **13**, 6009 (1997)
17. P. Segrè, F. Liu, P. Umbanhowar, D. Weitz, Nature **409**, 594 (2001)
18. M. Yoldi, W. González-Viñas, M.C. Arcos, R. Sirera, J. Mater. Sci. **41**, 2965 (2006)
19. A. Mihi, M. Ocaña, H. Míguez, Adv. Mater. **18**, 2244 (2006)
20. C. Arcos, K. Kumar, W. González-Viñas, R. Sirera, K.M. Poduska, A. Yethiraj, Phys. Rev. E **77**, 050402(R) (2008)
21. A.S. Dimitrov, K. Nagayama, Langmuir **12**, 1303 (1996)
22. P. Jiang, J.F. Bertone, K.S. Hwang, V.L. Colvin, Chem. Mater. **11**, 2132 (1999)
23. M. Szekeres, O. Kamalin, R.A. Schoonheydt, K. Wostyn, K. Clays, A. Persoons, I. Dékáány, J. Mater. Chem. **12**, 3268 (2002)

24. M. Yoldi, C. Arcos, B.R. Paulke, R. Sirera, W. González-Viñas, E. Görnitz, Mat. Sci. Eng. C-Bio. S **28**, 1038 (2008)
25. M. Giuliani, W. González-Viñas, Phys. Rev. E **79**, 032401 (2009)
26. R. Shimmin, A. DiMauro, P. Braun, Langmuir **22**, 6507 (2006)
27. P. Kralchevsky, N. Denkov, Curr. Opin. Coll. Interf. Sci. **6**, 383 (2001)
28. M. Giuliani, Ph.D. thesis, University of Navarra (2010)
29. A.V. Delgado, F. González-Caballero, R.J. Hunter, L.K. Koopal, J. Lyklema, Pure Appl. Chem. **77**, 1753 (2005)
30. H. Verheijen, M. Prins, Langmuir **15**, 6616 (1999)
31. R. Hayward, D. Saville, I. Aksay, Nature **404**, 56 (2000)
32. A. Rogach, N. Kotov, D. Koktysh, J. Ostrander, G. Ragoisha, Chem. Mater. **12**, 2721 (2000)
33. M. Pichumani, W. González-Viñas (2010) (in preparation)